Author Manuscript

Author Manuscript

Author Manuscript

Author Manuscript

HHS Public Access

Author manuscript

Clin Cancer Res. Author manuscript; available in PMC 2018 August 17.

Published in final edited form as:

Clin Cancer Res. 2017 December 01; 23(23): 7263–7275. doi:10.1158/1078-0432.CCR-17-0831.

4-1BB agonist focuses CD8+ tumor-infiltrating T-cell growth into a distinct repertoire capable of tumor recognition in pancreatic cancer

Donastas Sakellariou-Thompson[1], **Marie-Andrée Forget**[1], **Caitlin Creasy**[1], **Vincent Bernard**[2,3], **Li Zhao**[4], **Young Uk Kim**[1], **Mark W. Hurd**[3], **Naohiro Uraoka**[5], **Edwin Roger Parra**[5], **Ya'an Kang**[6], **Christopher A. Bristow**[7], **Jaime Rodriguez-Canales**[5], **Jason B. Fleming**[6,†], **Gauri Varadhachary**[8], **Milind Javle**[8], **Michael J. Overman**[8], **Hector A. Alvarez**[2,3], **Timothy P. Heffernan**[7], **Jianhua Zhang**[4], **Patrick Hwu**[1], **Anirban Maitra**[2,3,5], **Cara Haymaker**[1,*], and **Chantale Bernatchez**[1,*]

[1]Department of Melanoma Medical Oncology, The University of Texas MD Anderson Cancer Center (MDACC), Houston, TX

[2]Department of Pathology, The University of Texas MDACC, Houston, TX

[3]Sheikh Ahmed Center for Pancreatic Cancer Research, The University of Texas MDACC, Houston, TX

[4]Department of Genomic Medicine, The University of Texas MDACC, Houston, TX

[5]Department of Translational Molecular Pathology, The University of Texas MDACC, Houston, TX

[6]Department of Surgical Oncology, The University of Texas MDACC, Houston, TX

[7]Insitute for Applied Cancer Science, The University of Texas MDACC, Houston, TX

[8]Department of Gastrointestinal Medical Oncology, The University of Texas MDACC, Houston, TX

Abstract

Purpose—Survival for pancreatic ductal adenocarcinoma (PDAC) patients is extremely poor and improved therapies are urgently needed. Tumor-infiltrating lymphocyte (TIL) adoptive cell therapy (ACT) has shown great promise in other tumor types, such as metastatic melanoma where overall response rates of 50% have been seen. Given this success and the evidence showing that T-cell presence positively correlates with overall survival in PDAC, we sought to enrich for $CD8^+$ TIL capable of autologous tumor recognition. Additionally, we explored the phenotype and TCR repertoire of the $CD8^+$ TIL in the tumor microenvironment.

Corresponding authors: Cara Haymaker: Department of Melanoma Medical Oncology, University of Texas, MDACC, Unit 904, 7455 Fannin, Houston, TX, 77054, Tel: 713-792-1458, chaymaker@mdanderson.org; Chantale Bernatchez: Department of Melanoma Medical Oncology, University of Texas, MDACC, Unit 904, 7455 Fannin, Houston, TX, 77054, Tel: 713-563-8830, cbernatchez@mdanderson.org.

*These authors are co-corresponding

†Current affiliation: Department of Gastrointestinal Oncology, H. Lee Moffitt Cancer Center & Research Institute, Tampa, FL

Conflict of Interest Disclosure: We have no competing interests to disclose.

Author Manuscript Author Manuscript Author Manuscript Author Manuscript

Experimental Design—We used an agonistic 4-1BB mAb during the initial tumor fragment culture to provide 4-1BB co-stimulation and assessed changes in TIL growth, phenotype, repertoire, and anti-tumor function.

Results—Increased $CD8^+$ TIL growth from PDAC tumors was achieved with the aid of an agonistic 4-1BB mAb. Expanded TIL were characterized by an activated but not terminally differentiated phenotype. Moreover, 4-1BB stimulation expanded a more clonal and distinct $CD8^+$ TIL repertoire than IL-2 alone. TIL from both culture conditions displayed MHC class I-restricted recognition of autologous tumor targets.

Conclusions—Co-stimulation with an anti-4-1BB mAb increases the feasibility of TIL therapy by producing greater numbers of these tumor-reactive T cells. These results suggest that TIL ACT for PDAC is a potential treatment avenue worth further investigation for a patient population in dire need of improved therapy.

Keywords

TIL; pancreatic ductal adenocarcinoma; 4-1BB/CD137; immunotherapy

INTRODUCTION

Pancreatic cancer is the third-highest cause of cancer-related death for men and women in the United States and is expected to become the second-leading cause of cancer mortality by 2030 (1,2). The majority (85%) of pancreatic cancer diagnoses are classified as pancreatic ductal adenocarcinoma (PDAC) (3). Patients afflicted with PDAC often present with late-stage cancer and face the poorest prognosis of all cancer types with a 5-year survival rate of around 6% (4). Despite efforts to improve treatment, surgery, chemotherapy, and chemoradiation remain the only options. These treatment strategies have shown limited effectiveness as most patients will recur within a year of treatment even after successful tumor resection (4,5). Therefore, there is a great need to broaden treatment options.

Immunotherapy has made a tremendous mark in the treatment of cancer, especially in the past decade. Its success was first observed in the treatment of metastatic melanoma with high-dose IL-2 and then more recently with agents that block CTLA-4 and PD-1 (checkpoint blockade) (6–8). These treatments were later transposed to non-small cell lung cancer and renal cell carcinoma (9–11). In PDAC, however, they have been ineffective with no objective response seen for treatment with anti-CTLA-4 and anti-PD-L1 (12,13). The lack of efficacy could be a result of the paucity of $CD3^+$ T-cell infiltrate (14). An alternative approach to overcome the limitation posed by the modest immune infiltrate in PDAC is the *ex vivo* amplification of TIL for re-infusion through autologous ACT.

TIL ACT expands T cells up to several hundred-fold from surgically resected tumor and re-infuses them into the patient, providing a large influx of anti-tumor T cells. Our group and others have demonstrated its effectiveness in melanoma (15–18). With an average objective-response rate (ORR) of 51%, TIL ACT is among the best treatment options for metastatic disease. The MDACC experience also demonstrated a positive correlation between $CD8^+$ TIL infused and response (17). These results have already spurred efforts to translate ACT to

Author Manuscript Author Manuscript Author Manuscript Author Manuscript

other cancer types such as cervical (33% ORR), and gastrointestinal (25% ORR) (19,20). PDAC could also potentially benefit from TIL ACT as the presence of $CD8^+$ TIL is associated with greater 5-year survival (21,22). This suggests that endogenous PDAC TIL can exert some degree of tumor control, supporting the potential of TIL ACT.

One of the major challenges faced in growing TIL from GI cancer types for ACT trials is the difficulty of expanding $CD8^+$ T cells from the tumor tissue (23,24). PDAC has a well-characterized immunosuppressive tumor microenvironment that might contribute to the difficulty of triggering the proliferation of cytotoxic $CD8^+$ T cells from this tumor tissue and account for their decreased numbers (14,25). A method to resolve this barrier is by manipulating 4-1BB/CD137, a member of the tumor necrosis factor receptor family, which provides a strong co-stimulatory signal for increased activation, proliferation, and survival. This receptor is predominantly expressed on recently activated $CD8^+$ T cells with peak expression at 24 h (26). In fact, our group demonstrated that inclusion of an agonistic 4-1BB mAb (Urelumab, BMS) in TIL cultures was able to increase melanoma and triple-negative breast cancer $CD8^+$ TIL proliferation (27,28). Based on this previous work, we posited that use of an agonistic 4-1BB mAb in PDAC TIL culture would provide the same benefits of increased $CD8^+$ TIL yield.

Here, we demonstrate that the addition of an agonistic 4-1BB mAb increases the ability to grow TIL from PDAC, improves the total yield, and stimulates the proliferation of more $CD8^+$ T cells without overly differentiating them. In addition, these $CD8^+$ TIL have a distinct repertoire compared to IL-2 only grown TIL and display MHC class I-restricted autologous tumor recognition. These results support the use of 4-1BB-expanded TIL in ACT strategies for patients with PDAC.

MATERIALS AND METHODS

Patient selection

After obtaining informed consent, 26 patients with primary or metastatic pancreatic ductal adenocarcinoma underwent surgical resection. Two patients underwent resection on two sites, therefore a total of 28 samples were analyzed from 26 patients. Further patient characteristics are summarized in Supplementary Table S1. Patients are referred to by their de-identified “MP” number. In 23 patients, prior chemotherapy and/or chemoradiation was administered. Tissue from surgical resections was used to expand TIL under protocols (PA15-0176, LAB00-396, PA15-0014 for PDAC samples and LAB06-0755 for melanoma samples) approved by the Institutional Review Board of The University of Texas MD Anderson Cancer Center. This study was carried out in compliance with Good Clinical Practice concerning medical research in humans, as described in the Declaration of Helsinki.

Reagents and cell lines

A fully human and purified IgG4 monoclonal antibody (mAb) against human CD137/4-1BB, Urelumab (663513), was kindly provided by Bristol-Myers Squib (BMS). Human recombinant interleukin-2 (IL-2) (Proleukin™) was generously provided by Prometheus Therapeutics & Diagnostics. MHC class I blocking antibody (clone W6/32) and

Author Manuscript Author Manuscript Author Manuscript Author Manuscript

isotype control (mouse IgG2a, clone eBM2a) were purchased from Invitrogen and eBioscience, respectively. CAPAN-1 cell line was purchased from ATCC. Autologous tumor targets were found to match the patients using STR DNA fingerprinting performed at MDACC and the tumoroid was confirmed mycoplasma-free.

Isolation and expansion of TIL from human PDAC and metastatic melanoma tumors

The tumor samples were cut into 1-3 mm^2 fragments and placed in TIL culture media [TIL-CM: RPMI-1640 with GlutaMax (Gibco/Invitrogen), 1× Pen–Strep (Gibco/Invitrogen), 50 μmol/L 2-mercaptoethanol (Gibco/Invitrogen), 20 μg/mL Gentamicin (Gibco/Invitrogen), and 1 mmol/L pyruvate (Gibco/Invitrogen] with 6000 IU/ml IL-2 in 24-well plates for a period of 4 weeks, as previously described (17,29). The same method was applied for the metastatic melanoma samples. For the 4-1BB condition, both 6000 IU/ml IL-2 and 10 ug/ml 4-1BB mAb were added in the culture plates on day 0 and day 4 or 5. TIL were expanded for up to 35 days prior to performing the described assays or the rapid expansion protocol (REP). The REP was performed in the G-Rex 10 device (Wilson Wolf Manufacturing) following a scaled-down version of the previously described protocol (29). Briefly, TIL were put in culture with pooled allogeneic irradiated PBMC feeder cells at a ratio of 1 TIL to 200 feeders in combination with 6000U/ml IL-2 and 30ng/mL of anti-CD3 (OKT3 clone) on day 0 of the REP. The REP process lasted for 14 days, with REP-CM (half TIL-CM and half AIM-V (Invitrogen)) used for the first 7 days and only AIM-V for the last 7 days of expansion.

Immunohistochemistry (IHC)

Four-micrometer-thick serial sections were obtained from representative formalin-fixed, paraffin-embedded (FFPE) blocks for IHC, as well as hematoxylin and eosin (H&E) staining. H&E slides were examined by a pathologist to confirm the presence of tumor. IHC was performed using a Leica Bond Max automated staining system (Leica Microsystems) with antibodies against CD3 (dilution 1:100; Dako). The expression of the marker was detected using a Leica Bond Polymer Refine Detection kit (Leica Microsystems) with diaminobenzidine reaction to detect antibody labeling. Counterstaining was done using hematoxylin. Human tonsil FFPE tissues with and without CD3 primary antibody were used as positive and negative controls, respectively. For quantification of CD3 expression, the slides were digitally scanned at 200 magnification using the Aperio AT2 scanner (Leica Microsystems). The images were visualized using the ImageScope software (Leica Microsystems) and analyzed using the Aperio Image Toolbox (Leica Microsystems). Five regions of interests were randomly selected within the tumor area of each slide. The number of CD3 positive cells per mm^2 (cell density) was evaluated, and the final score was expressed as the average density of the five areas.

Flow Cytometric Analysis of TIL

Fresh tumor samples were manually disaggregated between frosted-glass slides to obtain a single-cell suspension for analysis. Both the disaggregated tissue samples and expanded TIL were stained in FACS Wash Buffer (Dulbecco’s Phosphate Buffered Saline 1× with 1% Bovine Serum Albumin) for 30 min using fluorochrome-conjugated monoclonal antibodies for CD3, CD4, CD8, CD16, CD56, CD57, Granzyme B, TBET, γδ TCR, CD27, CD28,

Author Manuscript Author Manuscript Author Manuscript Author Manuscript

CD45, CD45RA, CD45RO, CCR7, BTLA (clone J168) (BD Bioscience), PD-1, KLRG1 (Biolegend), and Eomes (eBioscience/ThermoFisher). Stained cells were fixed in 1% paraformaldehyde solution for 20 min. Intracellular staining was performed using eBioscience transcription factor staining kit according to the manufacturer's instructions. Samples were acquired using the BD FACSCanto™ II or BD LSRFortessa X-20 and analyzed using FlowJo Software v10.2 (Tree Star). Dead cells were excluded using an AQUA or Yellow live/dead staining (Invitrogen).

T-cell Receptor Beta Sequencing

Genomic DNA was extracted from samples using DNeasy Blood & Tissue Kit (Qiagen) as per manufacturer's instructions. TCRβ CDR3 regions were amplified from between 0.2–3 μg of DNA. All samples had the ImmunoSEQ™ assay performed at Adaptive Biotechnologies, with deep sequencing for PBMC DNA and survey-level sequencing for all others. Data analysis was performed at MDACC.

Recognition Assay via 4-1BB Upregulation and IFN-γ secretion

In order to provide greater cell numbers for functional assays, sorted $CD8^+$ TIL underwent the REP process. In triplicate, T cells were then put at a 10:1 ratio with their autologous tumor target, CAPAN-1(HLA mismatch control), or media (TIL alone). For some experiments the autologous tumor targets were incubated with 80 μg/ml of anti-MHC class I antibody (clone W6/32) for 3h prior to addition of T cells, as previously described (30). After 24 h incubation, the supernatants and T cells were collected. TIL were analyzed for 4-1BB/CD137 expression via flow cytometry. Detection of secreted cytokines in the corresponding supernatants were detected using a V-PLEX Plus Proinflammatory Panel 1 (human) kit and analyzed on a QuickPlex SQ 120, both available from Meso Scale Discovery. Reported values have CVs <20%.

Statistical Analysis

GraphPah Prism v6.0 (GraphPad Software) was used for graphing and statistical analysis. Differences between groups or experimental conditions were determined using either parametric or non-parametric, two-tailed t-tests (paired or unpaired) as appropriate. Linear regression and Spearman correlation analyses were also used as indicated. Two-sided *p*-values <0.05 were considered statistically significant and in the figures are indicated as * p<0.05, ** p<0.01, *** p<0.001, and **** p<0.0001.

RESULTS

PDAC TIL infiltrate is predominantly $CD4^+$ T-cells

To determine if the immune component of PDAC was sufficient for TIL ACT, we assessed the immune infiltrate by performing flow cytometry on manually disaggregated samples (n=28). The amount of $CD3^+$ TIL observed was less than 1% of all cells in the tumor sample on average as compared to metastatic melanoma with an $CD3^+$ TIL infiltrate >2% (Fig. 1A). Quantitative IHC analysis found that the mean density of $CD3^+$ TIL was 314 cells/mm^2 (Fig. 1B). This is fewer than what the literature reports for an immunogenic cancer like melanoma (422 cells/mm^2) (31). Additionally, metastatic (closed circle) and primary (open

Author Manuscript Author Manuscript Author Manuscript Author Manuscript

circle) PDAC samples did not appear to stratify. Further IHC analysis showed that all samples displayed ≥50% MHC Class I expression that was homogenous throughout the tumor tissue, suggesting that lack of Class I was not the reason for low $CD3^+$ infiltration (Fig. 1C). We also evaluated the proportion of $CD8^+$ and $CD4^+$ T cells. With an average CD8:CD4 ratio of 0.75, $CD4^+$ TIL comprised the majority of the T-cell infiltrate (Fig. 1D). As a point of comparison, metastatic melanoma showed a CD8:CD4 ratio of 1.5 (Fig. 1D). This ratio is similar to IHC data also from Erdag *et al.* that exhibited a CD8:CD4 ratio of 1.6 (31). Metastatic and primary sites did not seem to show a difference in CD8:CD4 ratio. Phenotypic analysis on the $CD8^+$ T cells determined their activation and differentiation state by assessing their expression of CD28 (50% ± 20%), CD45RA (10% ± 6%), PD-1 (45% ± 12%), and BTLA (20% ± 12%) (Fig. 1E). There were not enough primary samples that could be compared with metastatic samples to discern a difference in the phenotype of their TIL. However, the low frequency of CD45RA expression combined with expression levels of the other three markers suggests a relatively activated and not terminally-differentiated immune infiltrate.

PDAC shows an enriched T-cell repertoire in the tumor

Enrichment of T-cell clones at the tumor site in comparison to the blood would suggest that the patient is mounting an immunogenic response to its tumor and that specific T-cell clones are migrating to the tumor and proliferating in the tissue. To determine the tissue-specific distribution of the T-cell repertoire, we sequenced the T-cell receptor beta-chain (TCRB) CDR3 region of the T cells present in the blood, tumor and normal tissue from seven patients when available (Fig. 2). This analysis, presented as productive clonality, revealed that the T-cell repertoire in the tumor is generally more clonal than in the blood (Fig. 2A). Productive clonality is a measure of the degree to which one or several unique clones dominate the repertoire (32). Linear regression analysis compared the relative frequencies of individual TCRB clones present in both the blood and the tumor (Fig. 2B). All autologous blood-tumor pairs displayed slopes (m) <1, demonstrating a higher frequency of shared clones in the tumor than the blood. However, it is possible that high frequency clones present in the blood may correlate with high frequency clones present in the tumor. To determine the strength of correlation between clones in these sites, clones were partitioned and compared as follows using Spearman correlation: top clone frequency defined as ≥ 0.24% in the tumor (red circles), remaining clones partitioned in half with mid-frequency shared clones (green circles) and low-frequency shared clones (blue circles). Interestingly, Spearman correlation analysis showed weak or undefined correlation between the frequency of T-cell clones in the blood and their frequency in the tumor tissue (r_s <0.5), even among the top ranking clones in the tumor (red circles). Additionally, there were a few instances where the middle-ranking clones in the tumor (green circles) had greater correlation with their frequencies in the blood. Only MP31 showed good correlation (r_s = 0.61) of the frequencies of these top shared clones (Fig. 2B). Linear regression analysis was also used to compare the relative frequencies of individual TCRB clones present in both the normal and tumor tissue (Fig. 2C). Similar to the tumor-blood pairs, the slopes for all the tumor-normal tissue pairs were <1, indicating that individual shared clones were found at higher frequencies in the tumor than the normal. In addition, clones were partitioned and correlation calculated in the same manner as in the tumor-blood pairs described above. In contrast to the tumor-blood pairs, the

Author Manuscript Author Manuscript Author Manuscript Author Manuscript

frequencies of the T cells in autologous tumor-normal tissue pairs showed stronger correlation among the top and mid-frequency clones. Four of the five pairs (MP64B, MP75, MP81, and MP84B) had $r_s > 0.44$ while two of them (MP64B and M75) had $r_s > 0.5$, showing that the repertoires were very similar between the tumor and the normal tissue in these cases. Also different from the tumor versus blood comparison was the observation that the top ranking clones in the tumor (red circles) were often high ranking in the normal tissue as shown by clustering along the hashed line. MP31 shared no top clones and very few clones overall, so it was not partitioned.

Use of 4-1BB mAb increases total TIL growth, success rate, and frequency of $CD8^+$ TIL

Prior work by our group detailed how infusion of melanoma patients with a higher proportion of $CD8^+$ T cells and larger amount of TIL in general correlated with better clinical response (17). This result coupled with our observations of a predominance of $CD4^+$ TIL and relative scarcity of $CD3^+$ infiltration in general prompted us to consider ways to generate greater TIL growth that was rich in $CD8^+$ T cells. Previous work showed that recently antigen-activated $CD3^+CD8^+$ TIL upregulate expression of the costimulatory molecule 4-1BB (26). Furthermore, additional work by our group and others demonstrated that stimulation of this pathway through the use of an agonistic anti-4-1BB antibody could decrease time of TIL culture while increasing total TIL growth, particularly that of $CD3^+CD8^+$ T cells (24,27). Thus we set up samples for TIL culture where one set of fragments received only the conventional high-dose IL-2 (n=28) and the other received high-dose IL-2 plus the 4-1BB agonistic mAb (a4-1BB) (n=27) (Supplementary Table S2). The addition of a4-1BB increased the average total TIL growth from 40×10^6 cells for IL-2 alone to 100×10^6 for IL-2 + a4-1BB (Fig. 3A). Only cultures that grew in at least one of the two conditions are represented in Figure 3A. Additionally, a4-1BB doubled the success rate (14/27; 52%) for TIL growth from fragments compared to IL-2 only (8/28; 29%) (data summarized in Supplementary Table S3). The benchmark for a successful TIL culture, 12×10^6 total cells, was established from scaling down the MDACC Clinical Melanoma TIL Lab's criterion for success where 20 fragments are set up for TIL expansion and 40×10^6 cells is considered the minimum to treat a patient. Some IL-2 only cultures did not reach the benchmark and several produced no discernible TIL growth while their companion a4-1BB culture produced $\geq12\times10^6$ cells (Supplementary Table S2). To that effect, our work demonstrates that use of a 4-1BB mAb could rescue cultures that would not have grown under the conventional methods.

Next, we determined whether the cells that grew out of the cultures treated with a4-1BB were enriched for $CD3^+$ TIL and if $CD8^+$ TIL now comprised the majority of $CD3^+$ T cells. In cultures treated with a4-1BB, the total number of $CD3^+$ TIL was significantly increased over IL-2 only cultures on average from 30×10^6 cells to 75×10^6 cells respectively (Fig. 3B). Only cultures that grew in at least one of the two conditions are represented in Figure 3B. Since NK cells and $\gamma\delta$ TCR^+ T cells can also express 4-1BB, we stained for their presence in primary cultures to determine if the a4-1BB antibody being used was stimulating their growth (33,34). Indeed we found that three cultures with a4-1BB were enriched with a $CD3^-CD56^+$ population that was a greater proportion of the culture than $CD3^+$ TIL (Fig. 3C). Likewise, some cultures also showed an increase in $\gamma\delta$ TCR^+ T cells in a4-1BB

Author Manuscript Author Manuscript Author Manuscript Author Manuscript

cultures versus IL-2 alone (Fig. 3D, top graph). Only cultures that grew in both conditions are represented in Figures 3C and D. Neither the increase in NK cell growth ($p = 0.203$) or γδ TCR^+ T-cell growth ($p = 0.078$) due to 4-1BB co-stimulation was found to be significant overall. However, co-stimulation with a4-1BB produced a primary TIL culture that was on average 55% $CD3^+CD8^+$ TIL and 5% $CD4^+$ TIL. We observed the opposite situation in IL-2 alone cultures where 25% of $CD3^+$ TIL were $CD8^+$ and 60% were $CD4^+$. Overall, the 4-1BB mAb caused a dramatic switch in the composition of $CD3^+$ TIL towards the more favorable $CD8^+$ TIL (Fig. 3D).

Addition of 4-1BB mAb does not overly differentiate $CD8^+$ TIL

To better understand what effect the augmented growth via 4-1BB mAb stimulation had on $CD8^+$ TIL differentiation, we performed phenotypic analysis of CD28, CD45RA, PD-1, and BTLA expression. Between IL-2 only and a4-1BB cultures, the only significant change was a decrease in CD45RA expression ($p = 0.031$) (Fig. 4A). In fact, the level of expression of these markers was comparable to that seen on $CD8^+$ TIL in the fresh tumors (Fig. 1E). Further phenotyping was done using the established memory markers CD45RA, CD27, CD28, and CCR7 (Fig. 4B) (35). The vast majority of TIL, regardless of culture condition, were $CD45RA^-CCR7^-$, indicating that they are effector memory (EM) cells. Further characterization of their EM status was done by analyzing differential expression of CD27 and CD28, which has been shown to subdivide EM cells into four subsets termed EM1, EM2, EM3, and EM4 (Fig. 4C) (36).The majority of TIL, again regardless of culture condition, fell in the EM3 (CD27-CD28-) subset which Romero et al. have shown to display stronger cytolytic activity (36). We also further explored the degree of differentiation with the expression of KLRG1, CD57, Eomes, T-bet and Granzyme B. As shown in Supplementary Figure S1, KLRG1 was absent from both culture conditions. Combined with the other markers, this supplementary analysis further testifies that the stimulation of 4-1BB does not overly differentiate the cells and leads to the proliferation of effector/memory. Overall, this shows that even though a4-1BB stimulates aggressive expansion of activated $CD8^+$ TIL, they do not become overly or terminally differentiated.

Expansion of distinct $CD8^+$ T-cell clones favored by 4-1BB mAb compared to IL-2 alone

Next, we questioned how the culture conditions affected the repertoire of the TIL that grew out by sequencing sorted $CD8^+$ T cells and comparing their relative frequencies to each other and to their starting frequency in the tumor (Fig. 5). Many clones are shared (red lines) between the tumor and both TIL culture conditions. However, these clones are present at different frequencies between the conditions, as demonstrated by the position of the lines where further away from center denotes higher frequency. This shows that the addition of 4-1BB mAb favors expansion of unique clones as compared to IL-2 alone. This is further suggested by the presence of several T-cell clones that are shared between the tumor and only one of the culture conditions (blue lines). Finally, sequencing detected some clones that were not present in the tumor but were either present in only one culture (black lines) or shared only between the two culture conditions (green lines). Overall, in 4/5 patients, the addition of 4-1BB mAb in the culture expands a greater number of $CD8^+$ TIL but focuses their repertoire as evidenced by the smaller number of TIL clones in the a4-1BB cultures than the IL-2 alone cultures.

Author Manuscript Author Manuscript Author Manuscript Author Manuscript

PDAC CD8+ TIL recognize autologous tumor targets

Given the distinct repertoire generated by each culture condition, we assessed if the anti-tumor potential of both IL-2 only and IL-2 + a4-1BB cultured PDAC $CD8^+$ TIL differed. To this end, sorted $CD8^+$ TIL lines from both conditions were rapidly expanded (REP) and tested using a 24 h co-culture with autologous tumor targets derived from patients MP81 and MP64B (Fig. 6 and Supplementary Fig S2). Bulk TIL initially expanded using a4-1BB in combination with IL-2 were also put through the REP process and achieved the expected fold expansion (between 500 to 1500) after 14 days, confirming that both sorted $CD8^+$ and bulk populations could exponentially grow after being propagated with a4-1BB (Supplementary Fig. S2). Prior to co-culture setup, autologous tumor cells and CAPAN-1, a HLA-mismatched pancreatic tumor line for MP81, were stained for MHC class I expression (HLA-ABC) (Supplementary Fig. S3). Autologous tumor cells were found to express low, but detectable levels of MHC class I as compared to the CAPAN-1 cells (MFI: MP81 467, MP64B 606 vs 5387 for CAPAN-1). In spite of this low level of MHC class I expression, both IL-2 grown and a4-1BB grown MP81 TIL secreted more IFN-γ in the presence of the autologous target than with CAPAN-1(Fig. 6A). Upregulation of 4-1BB on $CD8^+$ T cells has been incorporated in tumor recognition assays previously (19,20). As such, both MP81 TIL lines significantly upregulated 4-1BB expression after exposure to the tumor target as compared to TIL co-cultured with CAPAN-1 (Fig. 6B and C). The upregulation of 4-1BB was particularly high on the $CD56^+$ T-cell subset, a cytotoxic T-cell subset (37). Given that the 4-1BB expression was higher in the $CD56^+$ $CD8^+$ MP81 TIL subset, we assessed MHC class I-restricted recognition by blocking MHC class I on the autologous tumor target for MP81 (Fig. 6D and E, left panels). We observed that most of the recognition (4-1BB upregulation) in the total $CD8^+$ population was MHC class I-restricted for TIL grown in both culture conditions. This experimental setup was repeated with an additional TIL and paired autologous tumor target (MP64B) with similar observations (Fig. 6D and E, right panels). CAPAN-1 was not used as a negative control for MP64B as it is partially HLA matched. Taken together, the IFN-γ secretion and elevated 4-1BB expression indicate there are MHC class I-restricted tumor-reactive $CD8^+$ T cells in the PDAC TIL repertoire.

DISCUSSION

In this study, we show that PDAC has a scarce, yet activated $CD8^+$ TIL infiltrate that is preferentially expanded with the addition of an agonistic 4-1BB mAb to the TIL culture. The 4-1BB mAb consistently augmented total TIL numbers and doubled the success rate of TIL growth without overly differentiating them in spite of the aggressive proliferation spurred by 4-1BB costimulation. Finally, despite the fact that the anti-4-1BB mAb favored expansion of distinct $CD8^+$ T-cell clones from the tumor in comparison to IL-2 alone, TIL derived with either culture condition showed tumor recognition via IFN-γ secretion and 4-1BB upregulation. While only two TIL lines and paired autologous tumor targets were able to be tested, we observed a higher frequency of anti-tumor reactive $CD8^+$ TIL in the a4-1BB grown cultures compared with TIL grown in IL-2 alone. These results suggest that the 4-1BB mAb can facilitate TIL ACT for PDAC by increasing the final yield of the desirable, anti-tumor $CD8^+$ T cells clones present in PDAC.

Author Manuscript Author Manuscript Author Manuscript Author Manuscript

PDAC has been characterized as an immunologically “cold” tumor due to the low presence of T cells, an immunosuppressive tumor infiltrate, the existence of dense stroma that supports tumor growth, and the lack of response to checkpoint blockade (12–14,25). However, this merits reconsideration as more recent work demonstrates that the presence of tertiary-lymphoid structures in pancreatic tumors and presence of TIL confer a survival advantage, suggesting the TIL are exerting a degree of tumor control (21,38–40). Our work adds to these findings by showing that these $CD8^+$ cells present in the fresh tumors have a desirable activation status and thus would be the type of TIL to exercise this tumor control. The low percentage of CD45RA (10% ± 6%) in general combined with PD-1 expression (45% ± 12%) suggests the population is mainly antigen-experienced but not terminally differentiated (41). Additionally, other work in melanoma has shown that PD-1 can identify the patient-specific $CD8^+$ tumor-reactive TIL, but further work is needed to confirm if this is also the case for PDAC (42).

Moreover, the lack of response to immune checkpoint blockade that contributes to the immunologically “cold” designation could be attributed to the paucity of $CD8^+$ TIL as shown by our work and others (21,38,43). Although the desmoplasia characteristic of PDAC is indicated as a physical barrier to TIL infiltration, it is curious that $CD8^+$ TIL are disproportionately affected. Pancreatic stellate cells (PSCs) in the surrounding stroma have already been implicated in the lack of $CD8^+$ TIL by sequestering them in the stroma, but we observed the same trend in liver metastases (44). Even though hepatic stellate cells (HSCs) reside in the liver and are very similar to PSCs, the question remains if HSCs have a similar effect (45). Could additional immunosuppressive mechanisms be in place that would result in the dearth of $CD8^+$ TIL in metastatic PDAC? The loss of MHC class I can be a mechanism of immune evasion by various tumors and that its loss is correlated with a decrease in $CD8^+$ TIL infiltration (46–48). However, we detected high MHC class I expression in all our tested samples, but cannot rule out the possible loss of a specific allele which this global assessment would not detect. Another possibility for the lack of $CD8^+$ TIL infiltration could be due to the relatively low amount of somatic mutations in PDAC (49). The fewer mutations could result in a less immunogenic tumor that does not stimulate as robust an immune response from effector T cells as has been suggested for multiple other tumor types (50). However, recent analysis of data from The Cancer Genome Atlas revealed that high T-cell cytolytic activity is not linked with increased mutational burden in PDAC (51). Further analysis is needed to better understand the reasons behind the low CD8-to-CD4 ratio in PDAC, although our proposed use of a 4-1BB mAb would address this issue for *in vitro* expansion.

TCR-sequencing of the T cells found in the blood, tumor, and TIL cultures provides further insight into the TIL population we are propagating from the tumor. Comparison between autologous tumor-blood and tumor-normal tissue pairs showed enrichment of shared T-cell clones in the tumor, again suggesting an ongoing immune response that would be atypical of a “cold” tumor. This data corroborates recent work which showed the same enriched T-cell repertoire in primary PDAC tumors versus the blood (38). While the T-cell clones found in the tumor were not enriched in the normal tissue for most patients, three normal tissue-tumor pairs (MP64B, MP75 and MP81) exhibited similarity between the frequencies of shared TIL clonotypes ($m>0.5$), particularly MP75. Furthermore, in all samples assessed by partitioning,

Author Manuscript Author Manuscript Author Manuscript Author Manuscript

the top clones shared between both sites exhibited a good correlation (r_s >0.44) as well as appeared to cluster along the hashed line in all but MP31. This suggests that high frequency clones found in the tumor are also found at high frequency in adjacent normal tissue. This observation is not true of the blood (i.e. high frequency clones in the tumor are not necessarily circulating at high frequency in the blood), nor are the lower frequency tumor-associated clones enriched in the blood. Altogether, this suggests that PDAC TIL are being pulled from a local, tissue-resident immune response as opposed to a systemic one.

While a4-1BB triggered massive expansion of $CD8^+$ TIL from tumor fragments, we did not observe any signs of further differentiation as the majority of the expanded TIL were effector memory cells lacking CD27 and CD28 (EM3). This subset has been described as highly cytotoxic and we do observe high levels of Granzyme B expressed in the TIL product (36). While we do detect CD57 expression on a4-1BB grown TIL, we do not detect any KLRG1 expression either, indicating that these cells are likely not senescent.

Our data show reactivity to autologous tumor targets, which builds upon the evidence for tumor-reactive TIL in PDAC as recently shown by other groups (24,38,52). The fact that many of the top clones detected in the expanded cultures were not top clones in the tumor and often were low frequency initially is notable. While Pasetto *et al.* demonstrated in melanoma that the clones that are enriched in the tumor tend to be highly tumor-reactive, our data indicate that low-frequency TIL have anti-tumor potential in PDAC as well (53). This suggestion is not without precedent since Tran *et al.* detected very low-frequency mutation-reactive TIL in GI tumors (19). Further analysis of the T-cell repertoires in each culture condition revealed that they favored expansion of distinct repertoires. These pre-REP repertoires were previously shown in melanoma to be conserved during the rapid expansion protocol (54). This result is consistent with the fact that the 4-1BB mAb selects recently activated TIL whereas IL-2 only provides a general T-cell growth signal. However, direct comparison of the clonal composition of the repertoires expanded in both culture conditions is not possible because of the unavoidable bias of tissue sampling introduced at the onset of the culture. Although the repertoires are different, TIL cultured under both conditions displayed tumor recognition.

In conclusion, the data display that metastatic PDAC harbors tumor-reactive TIL and the use of a 4-1BB mAb (Urelumab) can potentiate their expansion while preserving anti-tumor function. Although the 4-1BB costimulation doubles the growth success, it remains to be answered what factors prevent TIL outgrowth for 50% of samples despite their presence. Regardless, 4-1BB mAb use can enable ACT with bulk TIL by generating a focused, yet oligoclonal T-cell repertoire retaining diverse antigenic specificity mitigating the chances of tumor escape through antigen loss. Additionally, it is worth commenting that the effectiveness of TIL ACT in PDAC could be enhanced by combination with therapies that would target the immunosuppressive environment in the tumor and surrounding stroma. Ultimately, implementation of a 4-1BB mAb in TIL production would effectively double the number of patients eligible for therapy and provide a promising treatment option for metastatic disease.

Author Manuscript Author Manuscript Author Manuscript Author Manuscript

Supplementary Material

Refer to Web version on PubMed Central for supplementary material.

Acknowledgments

The authors would like to thank Alex Reuben for help with the hive plots, Feven Malu for help maintaining the tumoroid cell line, and Barbara Mino for help with IHC. We want to thank Bristol Myers Squibb for their generous contribution with the agonistic anti-4-1BB antibody, Urelumab (BMS-663513). Human recombinant interleukin-2 (IL-2) (Proleukin™) was generously provided by Prometheus Therapeutics & Diagnostics. Finally, the authors would like to thank the past and present MDACC TIL lab members: Orenthial J. Fulbright, Arely Wahl, Esteban Flores, Shawne T. Thorsen, René J. Tavera, Renjith Ramachandran and Audrey M. Gonzalez.

Funding: The study was supported by generous philanthropic contributions to The University of Texas MD Anderson Moon Shots Program. Additional support was provided by The University of Texas MD Anderson Cancer Center Support Grant (P30-CA16672) to the flow cytometry, research histology, and characterized cell line cores, the MDACC Institutional Tissue Bank, Multidisciplinary Research Proposal, and a supplement to this grant for the T-cell therapy program. Partial funding for maintenance of tumoroid cell line provided by the Cancer Prevention Research Institute of Texas (RP140106 to V.B.)

References

1. Siegel RL, Miller KD, Jemal A. Cancer statistics, 2015. CA Cancer J Clin. 2015; 65(1):5–29. DOI: 10.3322/caac.21254 [PubMed: 25559415]
2. Rahib L, Smith BD, Aizenberg R, Rosenzweig AB, Fleshman JM, Matrisian LM. Projecting cancer incidence and deaths to 2030: the unexpected burden of thyroid, liver, and pancreas cancers in the United States. Cancer Res. 2014; 74(11):2913–21. DOI: 10.1158/0008-5472.CAN-14-0155 [PubMed: 24840647]
3. Ryan DP, Hong TS, Bardeesy N. Pancreatic Adenocarcinoma. New England Journal of Medicine. 2014; 371(11):1039–49. DOI: 10.1056/NEJMra1404198 [PubMed: 25207767]
4. Kamisawa T, Wood LD, Itoi T, Takaori K. Pancreatic cancer. The Lancet. 2016; 388(10039):73–85. DOI: 10.1016/s0140-6736(16)00141-0
5. Neuzillet C, Tijeras-Raballand A, Bourget P, Cros J, Couvelard A, Sauvanet A, et al. State of the art and future directions of pancreatic ductal adenocarcinoma therapy. Pharmacology & Therapeutics. 2015; 155:80–104. DOI: 10.1016/j.pharmthera.2015.08.006 [PubMed: 26299994]
6. Hodi FS. Improved Survival with Ipilimumab in Patients with Metastatic Melanoma. N Engl J Med. 2010; 363(8)
7. Topalian SL, Sznol M, McDermott DF, Kluger HM, Carvajal RD, Sharfman WH, et al. Survival, durable tumor remission, and long-term safety in patients with advanced melanoma receiving nivolumab. J Clin Oncol. 2014; 32(10):1020–30. DOI: 10.1200/JCO.2013.53.0105 [PubMed: 24590637]
8. Larkin J, Chiarion-Sileni V, Gonzalez R, Grob JJ, Cowey CL, Lao CD, et al. Combined Nivolumab and Ipilimumab or Monotherapy in Untreated Melanoma. N Engl J Med. 2015; 373(1):23–34. DOI: 10.1056/NEJMoa1504030 [PubMed: 26027431]
9. Motzer RJ, Escudier B, McDermott DF, George S, Hammers HJ, Srinivas S, et al. Nivolumab versus Everolimus in Advanced Renal-Cell Carcinoma. N Engl J Med. 2015; 373(19):1803–13. DOI: 10.1056/NEJMoa1510665 [PubMed: 26406148]
10. Antonia S, Goldberg SB, Balmanoukian A, Chaft JE, Sanborn RE, Gupta A, et al. Safety and antitumour activity of durvalumab plus tremelimumab in non-small cell lung cancer: a multicentre, phase 1b study. Lancet Oncol. 2016; 17(3):299–308. DOI: 10.1016/S1470-2045(15)00544-6 [PubMed: 26858122]
11. Brahmer J, Reckamp KL, Baas P, Crino L, Eberhardt WE, Poddubskaya E, et al. Nivolumab versus Docetaxel in Advanced Squamous-Cell Non-Small-Cell Lung Cancer. N Engl J Med. 2015; 373(2):123–35. DOI: 10.1056/NEJMoa1504627 [PubMed: 26028407]

Author Manuscript Author Manuscript Author Manuscript Author Manuscript

12. Royal RE, Levy C, Turner K, Mathur A, Hughes M, Kammula US, et al. Phase 2 trial of single agent Ipilimumab (anti-CTLA-4) for locally advanced or metastatic pancreatic adenocarcinoma. J Immunother. 2010; 33(8):828–33. DOI: 10.1097/CJI.0b013e3181eec14c [PubMed: 20842054]
13. Brahmer JR. Safety and Activity of Anti–PD-L1 Antibody in Patients with Advanced Cancer. N Engl J Med. 2012; 366(6):2455–65. [PubMed: 22658128]
14. Koido S, Homma S, Takahara A, Namiki Y, Tsukinaga S, Mitobe J, et al. Current Immunotherapeutic Approaches in Pancreatic Cancer. Clinical and Developmental Immunology. 2011; 2011:1–15. DOI: 10.1155/2011/267539
15. Rosenberg SA, Yang JC, Sherry RM, Kammula US, Hughes MS, Phan GQ, et al. Durable complete responses in heavily pretreated patients with metastatic melanoma using T-cell transfer immunotherapy. Clin Cancer Res. 2011; 17(13):4550–7. DOI: 10.1158/1078-0432.CCR-11-0116 [PubMed: 21498393]
16. Besser MJ, Shapira-Frommer R, Treves AJ, Zippel D, Itzhaki O, Hershkovitz L, et al. Clinical responses in a phase II study using adoptive transfer of short-term cultured tumor infiltration lymphocytes in metastatic melanoma patients. Clin Cancer Res. 2010; 16(9):2646–55. DOI: 10.1158/1078-0432.CCR-10-0041 [PubMed: 20406835]
17. Radvanyi LG, Bernatchez C, Zhang M, Fox PS, Miller P, Chacon J, et al. Specific lymphocyte subsets predict response to adoptive cell therapy using expanded autologous tumor-infiltrating lymphocytes in metastatic melanoma patients. Clin Cancer Res. 2012; 18(24):6758–70. DOI: 10.1158/1078-0432.CCR-12-1177 [PubMed: 23032743]
18. Andersen R, Donia M, Ellebaek E, Borch TH, Kongsted P, Iversen TZ, et al. Long-Lasting Complete Responses in Patients with Metastatic Melanoma after Adoptive Cell Therapy with Tumor-Infiltrating Lymphocytes and an Attenuated IL2 Regimen. Clin Cancer Res. 2016; 22(15): 3734–45. DOI: 10.1158/1078-0432.CCR-15-1879 [PubMed: 27006492]
19. Tran E, Ahmadzadeh M, Lu YC, Gros A, Turcotte S, Robbins PF, et al. Immunogenicity of somatic mutations in human gastrointestinal cancers. Science. 2015; 350(6266):1387–90. DOI: 10.1126/science.aad1253 [PubMed: 26516200]
20. Stevanovic S, Draper LM, Langhan MM, Campbell TE, Kwong ML, Wunderlich JR, et al. Complete regression of metastatic cervical cancer after treatment with human papillomavirus-targeted tumor-infiltrating T cells. J Clin Oncol. 2015; 33(14):1543–50. DOI: 10.1200/JCO.2014.58.9093 [PubMed: 25823737]
21. Ino Y, Yamazaki-Itoh R, Shimada K, Iwasaki M, Kosuge T, Kanai Y, et al. Immune cell infiltration as an indicator of the immune microenvironment of pancreatic cancer. Br J Cancer. 2013; 108(4): 914–23. DOI: 10.1038/bjc.2013.32 [PubMed: 23385730]
22. Fukunaga A, Miyamoto M, Cho Y, Murakami S, Kawarada Y, Oshikiri T, et al. CD8+ Tumor-Infiltrating Lymphocytes Together with CD4+ Tumor-Infiltrating Lymphocytes and Dendritic Cells Improve the Prognosis of Patients with Pancreatic Adenocarcinoma. Pancreas. 2004; 28(1):e26–e31. DOI: 10.1097/00006676-200401000-00023 [PubMed: 14707745]
23. Turcotte S, Gros A, Hogan K, Tran E, Hinrichs CS, Wunderlich JR, et al. Phenotype and function of T cells infiltrating visceral metastases from gastrointestinal cancers and melanoma: implications for adoptive cell transfer therapy. J Immunol. 2013; 191(5):2217–25. DOI: 10.4049/jimmunol.1300538 [PubMed: 23904171]
24. Hall M, Liu H, Malafa M, Centeno B, Hodul PJ, Pimiento J, et al. Expansion of tumor-infiltrating lymphocytes (TIL) from human pancreatic tumors. J Immunother Cancer. 2016; 4:61.doi: 10.1186/s40425-016-0164-7 [PubMed: 27777771]
25. Wachsman M. Pancreatic Ductal Adenocarcinoma: A Review of Immunologic Aspects. J Investig Med. 2012; 60(4):643–63. DOI: 10.231/JIM.0b013e31824a4d79
26. Wolfl M, Kuball J, Ho WY, Nguyen H, Manley TJ, Bleakley M, et al. Activation-induced expression of CD137 permits detection, isolation, and expansion of the full repertoire of CD8+ T cells responding to antigen without requiring knowledge of epitope specificities. Blood. 2007; 110(1):201–10. DOI: 10.1182/blood-2006-11-056168 [PubMed: 17371945]
27. Chacon JA, Sarnaik AA, Chen JQ, Creasy C, Kale C, Robinson J, et al. Manipulating the tumor microenvironment ex vivo for enhanced expansion of tumor-infiltrating lymphocytes for adoptive cell therapy. Clin Cancer Res. 2015; 21(3):611–21. DOI: 10.1158/1078-0432.CCR-14-1934 [PubMed: 25472998]

Author Manuscript Author Manuscript Author Manuscript Author Manuscript

28. Harao M, Forget MA, Roszik J, Gao H, Babiera GV, Krishnamurthy S, et al. 4-1BB-enhanced expansion of CD8+ TIL from triple-negative breast cancer unveils mutation-specific CD8+ T cells. Cancer Immunol Res. 2017; doi: 10.1158/2326-6066.CIR-16-0364
29. Forget MA, Malu S, Liu H, Toth C, Maiti S, Kale C, et al. Activation and propagation of tumor-infiltrating lymphocytes on clinical-grade designer artificial antigen-presenting cells for adoptive immunotherapy of melanoma. J Immunother. 2014; 37(9):448–60. DOI: 10.1097/CJI.0000000000000056 [PubMed: 25304728]
30. Doucet JD, Forget MA, Grange C, Rouxel RN, Arbour N, von Messling V, et al. Endogenously expressed matrix protein M1 and nucleoprotein of influenza A are efficiently presented by class I and class II major histocompatibility complexes. J Gen Virol. 2011; 92(Pt 5):1162–71. DOI: 10.1099/vir.0.029777-0 [PubMed: 21307226]
31. Erdag G, Schaefer JT, Smolkin ME, Deacon DH, Shea SM, Dengel LT, et al. Immunotype and immunohistologic characteristics of tumor-infiltrating immune cells are associated with clinical outcome in metastatic melanoma. Cancer Res. 2012; 72(5):1070–80. DOI: 10.1158/0008-5472.CAN-11-3218 [PubMed: 22266112]
32. Robins HS, Campregher PV, Srivastava SK, Wacher A, Turtle CJ, Kahsai O, et al. Comprehensive assessment of T-cell receptor beta-chain diversity in alphabeta T cells. Blood. 2009; 114(19): 4099–107. DOI: 10.1182/blood-2009-04-217604 [PubMed: 19706884]
33. Lin W, Voskens CJ, Zhang X, Schindler DG, Wood A, Burch E, et al. Fc-dependent expression of CD137 on human NK cells: insights into "agonistic" effects of anti-CD137 monoclonal antibodies. Blood. 2008; 112(3):699–707. DOI: 10.1182/blood-2007-11-122465 [PubMed: 18519814]
34. Lee SJ, Kim YH, Hwang SH, Kim YI, Han IS, Vinay DS, et al. 4-1BB signal stimulates the activation, expansion, and effector functions of gammadelta T cells in mice and humans. Eur J Immunol. 2013; 43(7):1839–48. DOI: 10.1002/eji.201242842 [PubMed: 23640752]
35. Sallusto F, Geginat J, Lanzavecchia A. Central memory and effector memory T cell subsets: function, generation, and maintenance. Annu Rev Immunol. 2004; 22:745–63. DOI: 10.1146/annurev.immunol.22.012703.104702 [PubMed: 15032595]
36. Romero P, Zippelius A, Kurth I, Pittet MJ, Touvrey C, Iancu EM, et al. Four functionally distinct populations of human effector-memory CD8+ T lymphocytes. J Immunol. 2007; 178(7):4112–9. [PubMed: 17371966]
37. Correia MP, Costa AV, Uhrberg M, Cardoso EM, Arosa FA. IL-15 induces CD8+ T cells to acquire functional NK receptors capable of modulating cytotoxicity and cytokine secretion. Immunobiology. 2011; 216(5):604–12. DOI: 10.1016/j.imbio.2010.09.012 [PubMed: 20956026]
38. Poschke I, Faryna M, Bergmann F, Flossdorf M, Lauenstein C, Hermes J, et al. Identification of a tumor-reactive T-cell repertoire in the immune infiltrate of patients with resectable pancreatic ductal adenocarcinoma. Oncoimmunology. 2016; 5(12):e1240859.doi: 10.1080/2162402X.2016.1240859 [PubMed: 28123878]
39. Castino GF, Cortese N, Capretti G, Serio S, Di Caro G, Mineri R, et al. Spatial distribution of B cells predicts prognosis in human pancreatic adenocarcinoma. Oncoimmunology. 2016; 5(4):e1085147.doi: 10.1080/2162402X.2015.1085147 [PubMed: 27141376]
40. Hiraoka N, Ino Y, Yamazaki-Itoh R, Kanai Y, Kosuge T, Shimada K. Intratumoral tertiary lymphoid organ is a favourable prognosticator in patients with pancreatic cancer. Br J Cancer. 2015; 112(11):1782–90. DOI: 10.1038/bjc.2015.145 [PubMed: 25942397]
41. Legat A, Speiser DE, Pircher H, Zehn D, Fuertes Marraco SA. Inhibitory Receptor Expression Depends More Dominantly on Differentiation and Activation than "Exhaustion" of Human CD8 T Cells. Front Immunol. 2013; 4:455.doi: 10.3389/fimmu.2013.00455 [PubMed: 24391639]
42. Turcotte S, Gros A, Tran E, Lee CC, Wunderlich JR, Robbins PF, et al. Tumor-reactive CD8+ T cells in metastatic gastrointestinal cancer refractory to chemotherapy. Clin Cancer Res. 2014; 20(2):331–43. DOI: 10.1158/1078-0432.CCR-13-1736 [PubMed: 24218514]
43. Emmrich J. Typing of Leukocytes in Pancreatic Tissue Surrounding Human Pancreatic Carcinoma. Annals New York Academy of Sciences. 1999; 880:171–4.
44. Ene-Obong A, Clear AJ, Watt J, Wang J, Fatah R, Riches JC, et al. Activated pancreatic stellate cells sequester CD8+ T cells to reduce their infiltration of the juxtatumoral compartment of

Author Manuscript Author Manuscript Author Manuscript Author Manuscript

pancreatic ductal adenocarcinoma. Gastroenterology. 2013; 145(5):1121–32. DOI: 10.1053/j.gastro.2013.07.025 [PubMed: 23891972]

45. Buchholz M, Kestler HA, Holzmann K, Ellenrieder V, Schneiderhan W, Siech M, et al. Transcriptome analysis of human hepatic and pancreatic stellate cells: organ-specific variations of a common transcriptional phenotype. J Mol Med (Berl). 2005; 83(10):795–805. DOI: 10.1007/s00109-005-0680-2 [PubMed: 15976918]
46. Garcia-Lora A, Algarra I, Garrido F. MHC class I antigens, immune surveillance, and tumor immune escape. J Cell Physiol. 2003; 195(3):346–55. DOI: 10.1002/jcp.10290 [PubMed: 12704644]
47. Aptsiauri N, Cabrera T, Garcia-Lora A, Lopez-Nevot MA, Ruiz-Cabello F, Garrido F. MHC Class I Antigens and Immune Surveillance in Transformed Cells. 2007; 256:139–89. DOI: 10.1016/s0074-7696(07)56005-5
48. Al-Batran S. Intratumoral T-Cell Infiltrates and MHC Class I Expression in Patients with Stage IV Melanoma. Cancer Res. 2005; 65(9):3937–41. [PubMed: 15867394]
49. Alexandrov LB, Nik-Zainal S, Wedge DC, Aparicio SA, Behjati S, Biankin AV, et al. Signatures of mutational processes in human cancer. Nature. 2013; 500(7463):415–21. DOI: 10.1038/nature12477 [PubMed: 23945592]
50. Rooney MS, Shukla SA, Wu CJ, Getz G, Hacohen N. Molecular and genetic properties of tumors associated with local immune cytolytic activity. Cell. 2015; 160(1–2):48–61. DOI: 10.1016/j.cell.2014.12.033 [PubMed: 25594174]
51. Balli D, Rech AJ, Stanger BZ, Vonderheide RH. Immune cytolytic activity stratifies molecular subsets of human pancreatic cancer. Clin Cancer Res. 2016 In Press.
52. Meng Q, Liu Z, Rangelova E, Poiret T, Ambati A, Rane L, et al. Expansion of Tumor-reactive T Cells From Patients With Pancreatic Cancer. J Immunother. 2016; 39(2):81–9. DOI: 10.1097/CJI.0000000000000111 [PubMed: 26849077]
53. Tran E, Robbins PF, Lu YC, Prickett TD, Gartner JJ, Jia L, et al. T-Cell Transfer Therapy Targeting Mutant KRAS in Cancer. N Engl J Med. 2016; 375(23):2255–62. DOI: 10.1056/NEJMoa1609279 [PubMed: 27959684]
54. Forget MA, Haymaker C, Dennison JB, Toth C, Maiti S, Fulbright OJ, et al. The beneficial effects of a gas-permeable flask for expansion of Tumor-Infiltrating lymphocytes as reflected in their mitochondrial function and respiration capacity. Oncoimmunology. 2016; 5(2):e1057386.doi: 10.1080/2162402X.2015.1057386 [PubMed: 27057427]

Author Manuscript Author Manuscript Author Manuscript Author Manuscript

TRANSLATIONAL RELEVANCE

Pancreatic ductal adenocarcinoma (PDAC) has a dismal survival rate. Recent successes in tumor immunotherapy have not translated to PDAC. However, the presence of $CD8^+$ T cells in PDAC is correlated with greater survival. We hypothesize that systemic immunotherapy approaches do not successfully reactivate the anti-tumor immunity in PDAC and postulate that this may be overcome by ex-vivo expansion of Tumor-Infiltrating Lymphocytes (TIL) followed by adoptive transfer (ACT). The expression of the 4-1BB costimulatory molecule marks recently antigen-experienced $CD8^+$ TIL. We successfully used an agonistic GMP-grade 4-1BB mAb (Urelumab) added directly to the initial tumor fragment cultures to preferentially stimulate their growth. This method offers a feasible way to implement TIL ACT for PDAC by ensuring the large expansion of activated, tumor-specific $CD8^+$ TIL.

Author Manuscript
Author Manuscript
Author Manuscript
Author Manuscript

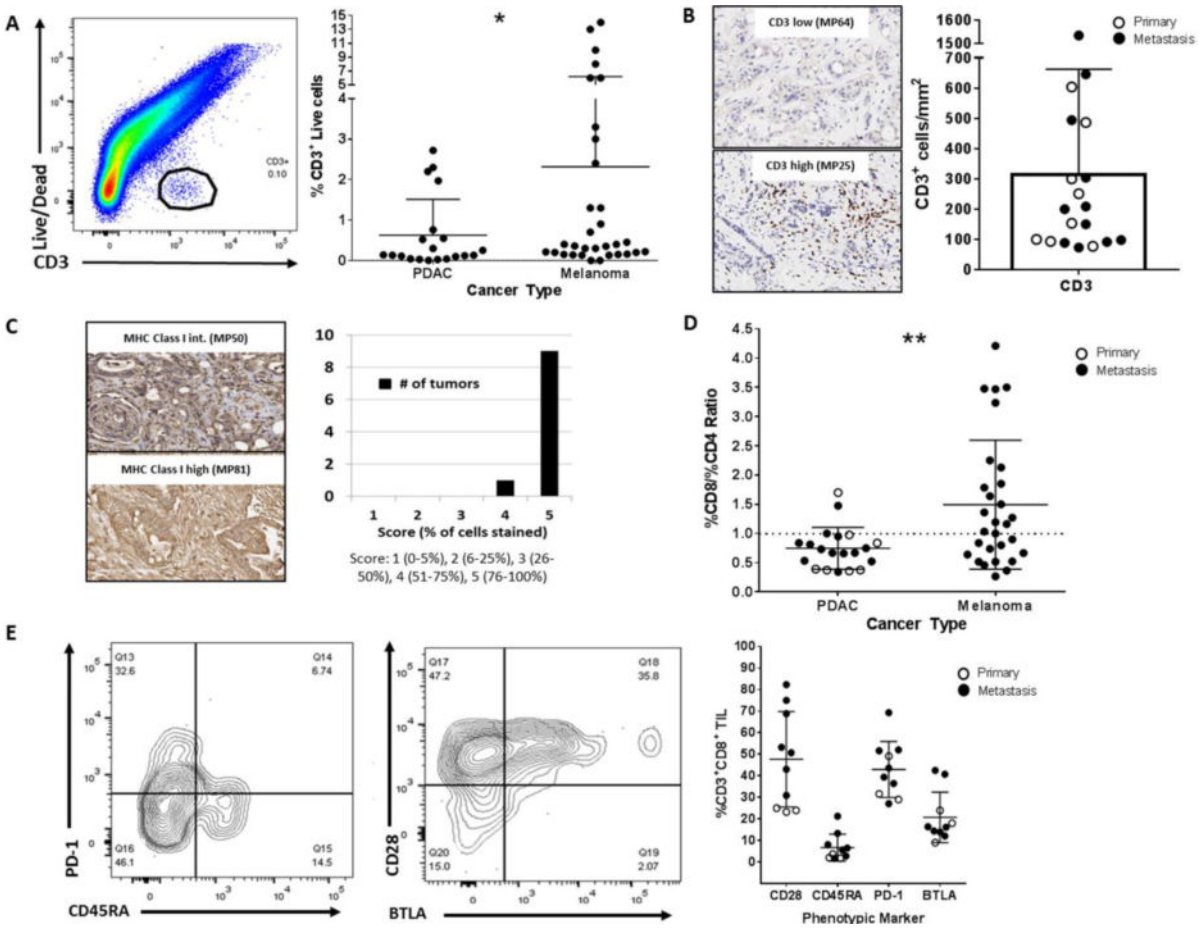

Figure 1. PDAC TIL infiltrate is largely dominated by CD4$^+$ T cells

(**A**) Flow cytometry analysis was performed on freshly disaggregated tumor samples. A representative figure showing the gating strategy based on CD3 and live/dead is presented on the left. The right graph shows a significantly lower CD3$^+$ immune infiltrate in PDAC as compared to metastatic melanoma. (**B**) IHC analysis quantified the amount of CD3$^+$ infiltration in PDAC. (**C**) IHC analysis showed that >75% of the PDAC tumor tissue expresses MHC class I demonstrating HLA Class I expression. (**D**) CD8/CD4 ratio in fresh PDAC sample compared to melanoma. (**E**) Phenotypic analysis of expression of CD28, CD45RA, PD1, and BTLA on CD8$^+$ TIL present in fresh samples.

Author Manuscript
Author Manuscript
Author Manuscript
Author Manuscript

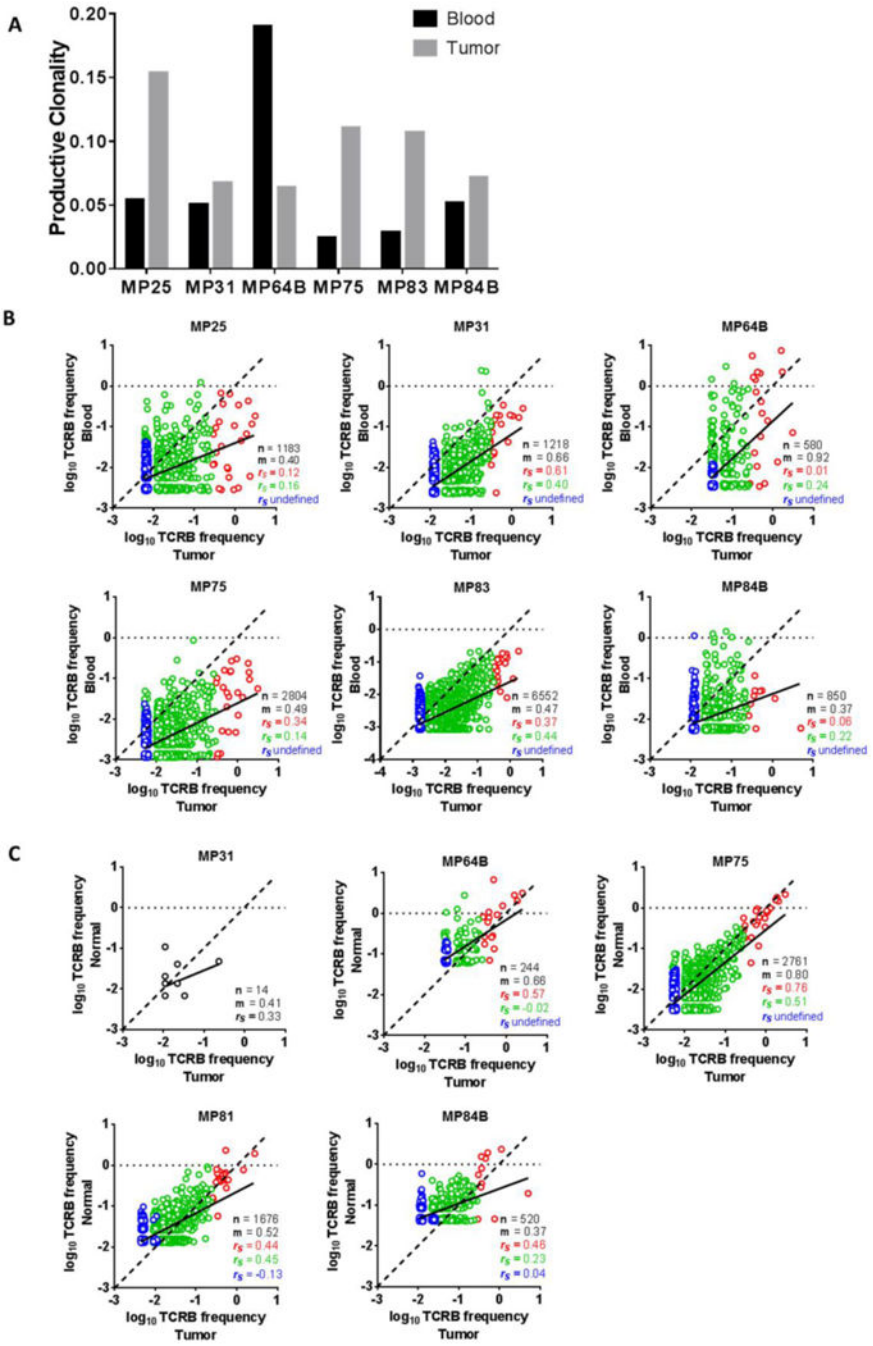

Figure 2. TCRB clonality and frequency of shared TCRB clones higher in tumor than autologous blood and normal tissue

CDR3 sequencing of the TCR beta-chain was done on the blood, tumor and normal tissue. (**A**) TCRB clonality is higher in the tumor than the blood for most samples. (**B**) Frequencies of shared clones in the tumor and blood and (**C**) tumor and normal tissue are shown. Top T-cell clones from the tumor that are also shared between the blood or normal tissue are highlighted in red. The remaining shared clones are split in half with the top half colored green and the bottom half colored blue. Shared clones (n), linear regression analysis with

line of best fit (solid line), slope of best-fit line (m), and color-coded Spearman correlation coefficient (r_S) for each group are next to each graph in (**B**) and (**C**). Hatched lines represent the identity line, i.e. 1:1 frequency ratio. The data plotted in (**B**) and (**C**) was jittered to prevent over-plotting.

Author Manuscript Author Manuscript Author Manuscript Author Manuscript

Author Manuscript Author Manuscript Author Manuscript Author Manuscript

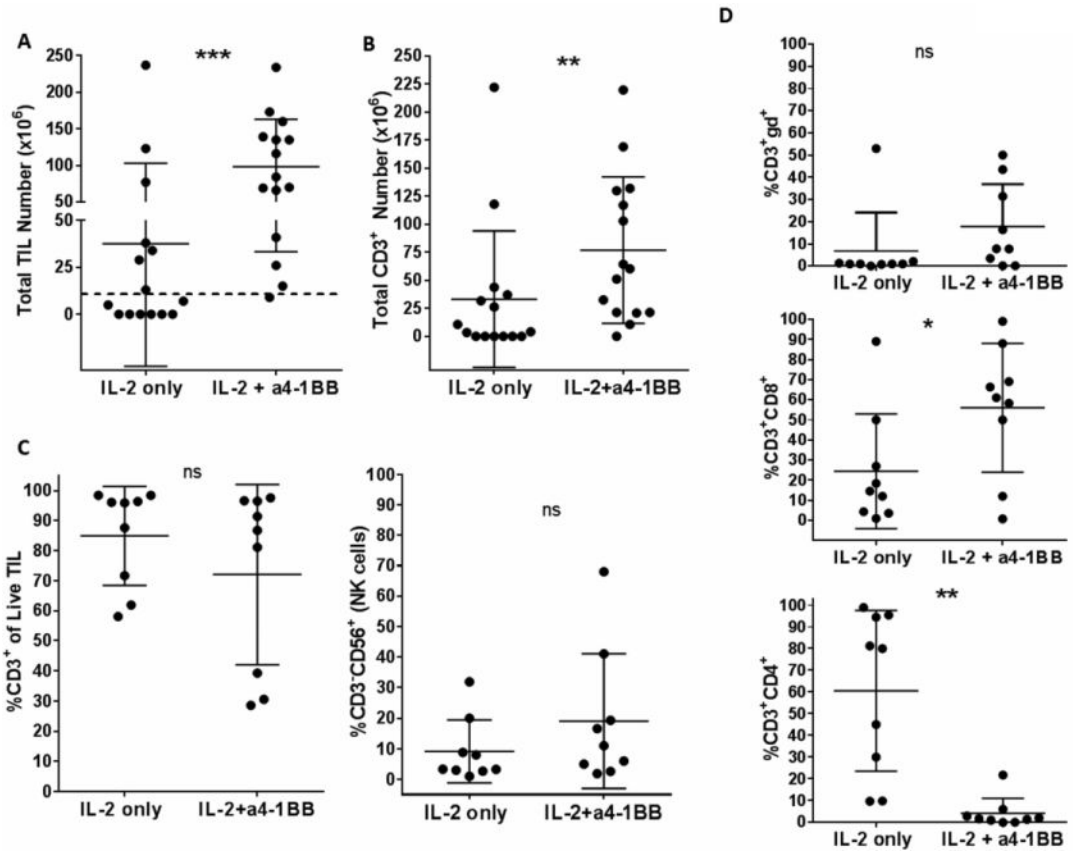

Figure 3. High numbers of CD8$^+$ TIL can be expanded from PDAC with the use of agonistic anti-4-1BB antibody

Tumor fragments were set up with either high dose of IL-2 alone or with the addition of an agonistic anti-4-1BB (a4-1BB). (**A**) Total TIL numbers and (**B**) total CD3$^+$ TIL expanded with or without a4-1BB. Expansion was considered successful with 12×10^6 cells or more (dotted line); cultures which did not reach this number in both conditions are not presented. (**C**) Percentage of CD3$^+$ and CD3$^-$ CD56$^+$ TIL grown in each condition. Only cultures with successful growth in both conditions are presented. (**D**) Percentage of γδ TCR$^+$, CD8$^+$, and CD4$^+$ within the CD3$^+$ T cell subset. Only cultures with successful growth in both conditions are presented.

Author Manuscript Author Manuscript Author Manuscript Author Manuscript

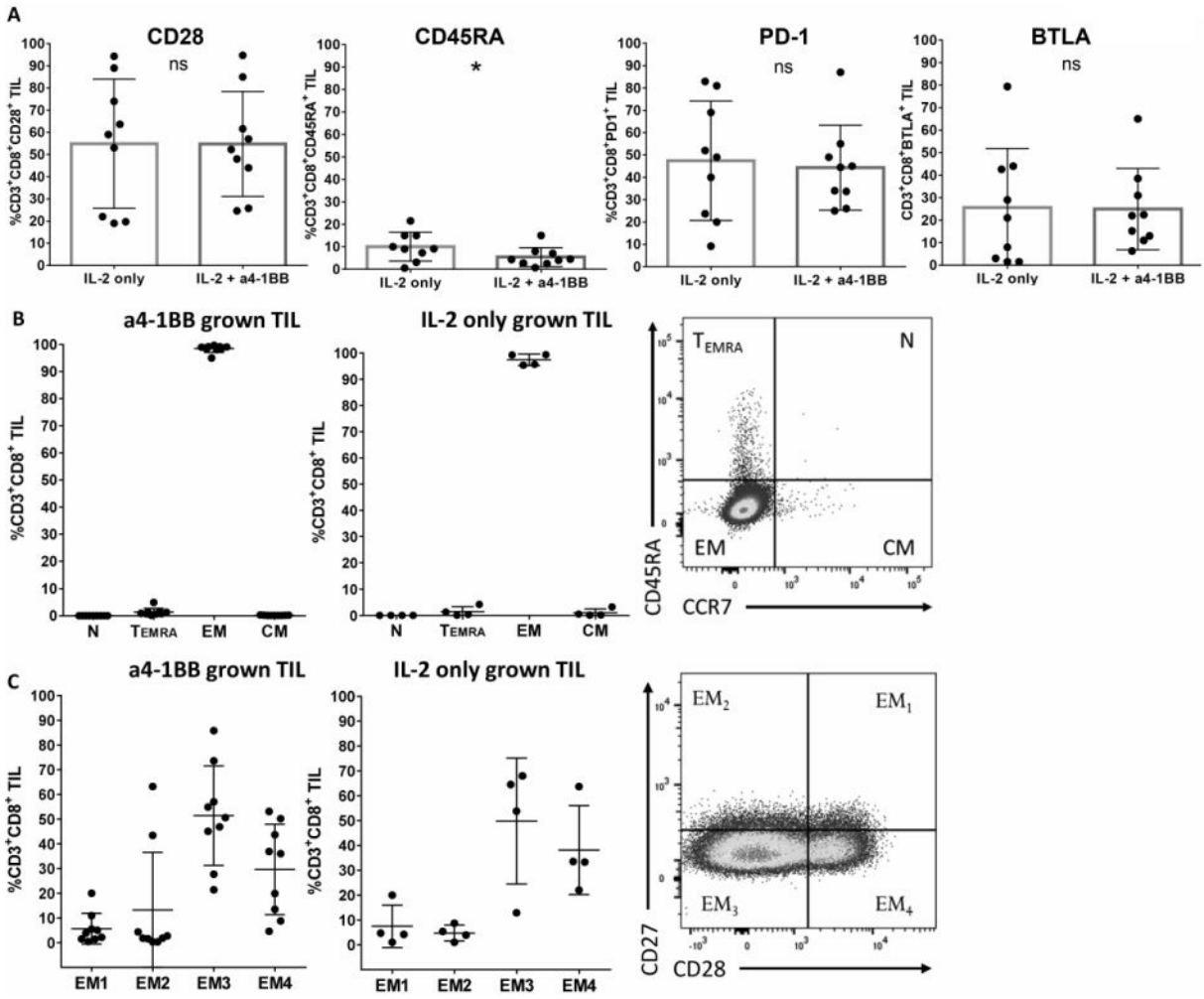

Figure 4. Addition of a4-1BB does not overly differentiate CD8$^+$ TIL. (A) Percent expression of phenotypic markers (CD28, CD45RA, PD1 and BTLA) for T-cell activation and differentiation on CD8$^+$ TIL post-culture evaluated by flow cytometry. **(B)** Comparing expression of CD45RA and CCR7 shows whether TIL are naïve (N), central memory (CM), effector memory (EM), or terminally differentiated effector memory that re-express CD45RA (T_{EMRA}). **(C)** Comparison of CD27 and CD28 expression shows EM subsets of CD8$^+$ TIL grown in each culture condition. Representative dot plots for **B** and **C** are shown on the right.

Author Manuscript Author Manuscript Author Manuscript Author Manuscript

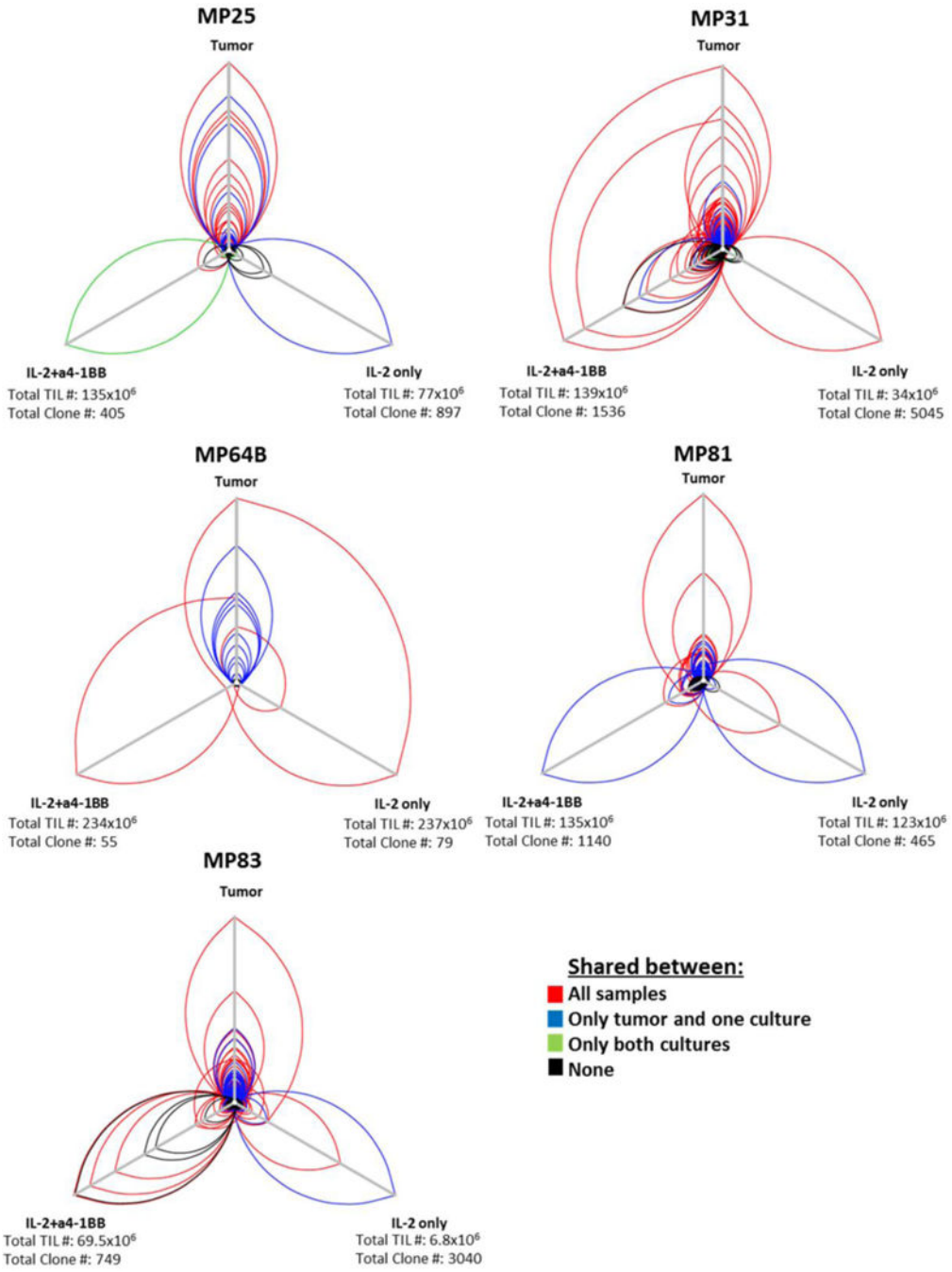

Figure 5. Distinct TCR repertoires are favored in each culture condition

CDR3 sequencing of the TCR beta-chain was done on the blood, tumor and expanded TIL ($CD8^+$ sorted). Relative frequency in each sample is indicated along each axis of the hive plot with frequency increasing away from the center. Red lines indicate TCRB clones shared between all three samples, blue lines for those shared between one culture condition and the tumor, green for those shared only between the culture conditions and finally black lines indicate TCRB clones found in only one condition. Total TIL grown and number of unique clones in each condition are shown.

Author Manuscript Author Manuscript Author Manuscript Author Manuscript

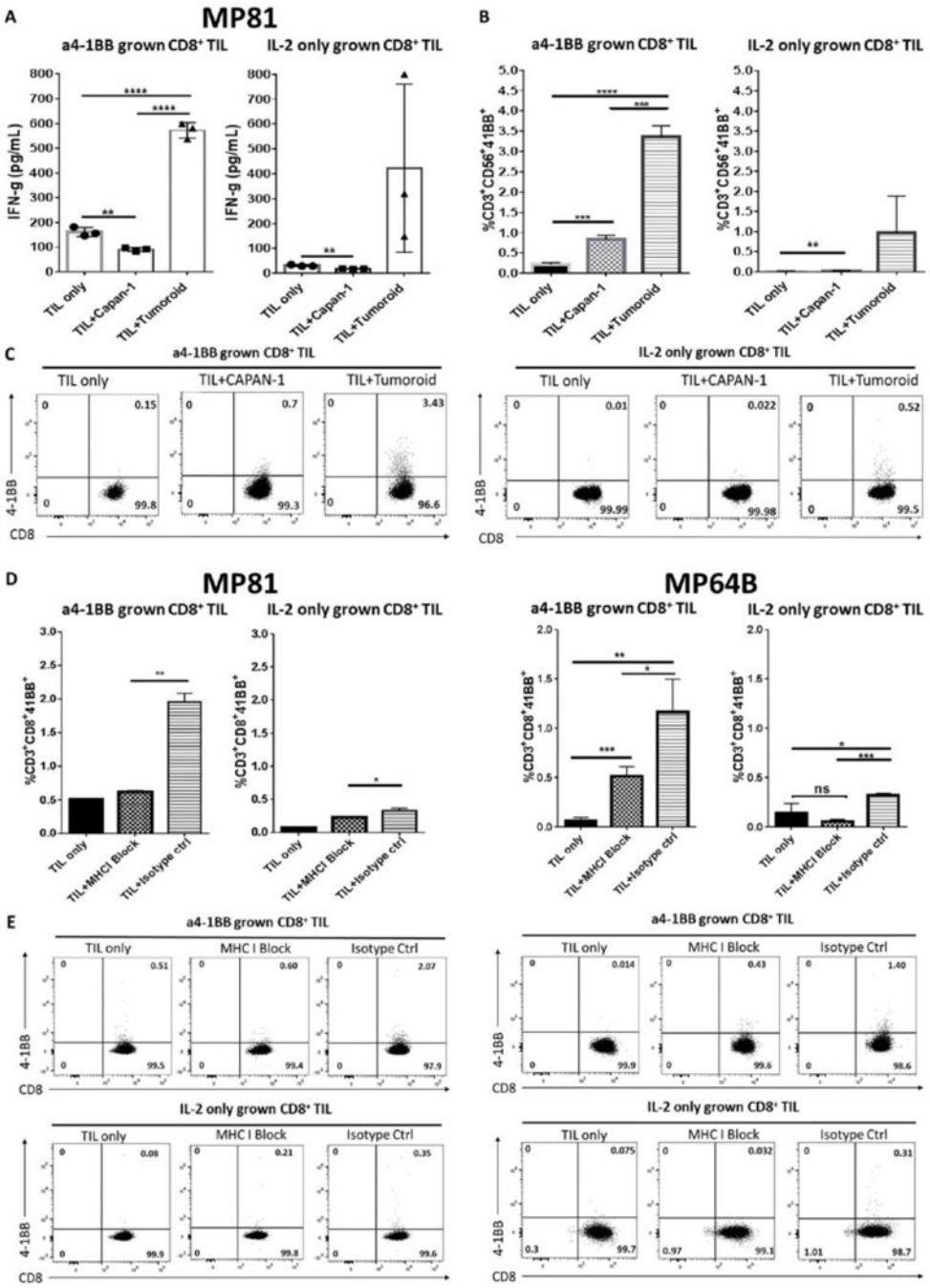

Figure 6. Reactivity of PDAC TIL to an autologous tumor target. (A-C)

Sorted MP81 $CD8^+$ TIL grown in IL-2+a4-1BB or IL-2 only were co-cultured for 24 h with autologous tumor, HLA-mismatched tumor line CAPAN-1, or media (TIL only). All conditions were in triplicate. **(A)** IFN-γ secretion was measured as well as **(B,C)** upregulation of 4-1BB on $CD56^+CD8^+$ TIL. Part **(B)** shows the compiled results of dot plot analysis of 4-1BB upregulation visualized by flow cytometry and **(C)** shows representative dot plots of 4-1BB upregulation. Results for a4-1BB grown TIL and IL-2 only grown TIL are from separate experiments. **(D,E)** Sorted MP81 $CD8^+$ TIL (left graphs) and **s**orted

Author Manuscript Author Manuscript Author Manuscript Author Manuscript

MP64B CD8$^+$ TIL (right graphs) grown in IL-2+a4-1BB or IL-2 only were co-cultured for 24 h with autologous tumor, pre-treated with MHC-I blocking antibody (W6/32) or isotype control (IgG2a), or media (TIL only). All conditions were in duplicate or triplicate. Part **(D)** shows the compiled results of dot plot analysis of 4-1BB upregulation visualized by flow cytometry for MP81 CD8$^+$ TIL (left graph) and MP64B CD8$^+$ TIL (right graph). **(E)** shows representative dot plots of 4-1BB upregulation.